

1 **Surface tension propulsion of fungal spores**

2
3 Xavier Noblin¹, Sylvia Yang², Jacques Dumais³

4
5 ¹Laboratoire de Physique de la Matière Condensée, CNRS -UMR 6622, Université de
6 Nice-Sophia-Antipolis, Parc Valrose, 06108 Nice Cedex 2, France

7
8 ²Department of Biology, University of Washington, Seattle, WA 98195, USA

9
10 ³Department of Organismic and Evolutionary Biology, Harvard University, Cambridge,
11 MA, 02138, USA

12
13 **Corresponding Author:**

14 Jacques Dumais

15 Department of Organismic and Evolutionary Biology

16 Harvard University

17 16 Divinity Ave (rm 1105)

18 Cambridge, MA, 02138, USA

19 Fax: 617 384-5874

20 Telephone: 617 496-0751

21
22 **Short Title:** Fungal Spore Ejection

23 **Keywords:** *Auricularia auricula* — ballistospores — wetting phenomena —
24 spore dispersal — surface tension

25
26 Manuscript pages: 25

27 Number of Tables: 2

28 Number of Figures: 8

29

1 **Summary**

2 Most basidiomycete fungi actively eject their spores. The process begins with the
3 condensation of a water droplet at the base of the spore. The fusion of the droplet onto the
4 spore creates a momentum that propels the spore forward. The use of surface tension for
5 spore ejection offers a new paradigm to perform work at small length scales. However, this
6 mechanism of force generation remains poorly understood. To elucidate how fungal spores
7 make effective use of surface tension, we performed a detailed mechanical analysis of the
8 three stages of spore ejection: the transfer of energy from the drop to the spore, the work of
9 fracture required to release the spore from its supporting structure, and the kinetic energy
10 of the spore after ejection. Highspeed video imaging of spore ejection in *Auricularia*
11 *auricula* and *Sporobolomyces* yeasts revealed that drop coalescence takes place over a
12 short distance ($\sim 5 \mu\text{m}$) and energy transfer is completed in less than $4 \mu\text{s}$. Based on these
13 observations, we developed an explicit relation for the conversion of surface energy into
14 kinetic energy during the coalescence process. The relation was validated with a simple
15 artificial system and shown to predict the initial spore velocity accurately (predicted
16 velocity: 1.2 m s^{-1} ; observed velocity: 0.8 m s^{-1} for *A. auricula*). Using calibrated
17 microcantilevers, we also demonstrate that the work required to detach the spore from the
18 supporting sterigma represents only a small fraction of the total energy available for spore
19 ejection. Finally, our observations of this unique discharge mechanism reveal a surprising
20 similarity with the mechanics of jumping in animals.

21

1 Introduction

2 Most basidiomycetes, including many edible mushrooms, actively disperse their spores
3 through a mechanism known as ballistospory (Buller, 1950; Ingold, 1939). The spores, or
4 ballistospores, are borne on the gills of mushroom caps or equivalent reproductive
5 structures (Fig. 1A). Each spore develops on an outgrowth known as the sterigma to which
6 it is attached via the hilum – a constriction of the sterigma that works as an abscission zone
7 (Fig. 1B,C). Spore ejection is preceded by the condensation of Buller’s drop at the hilar
8 appendix located on the proximal end of the spore (Fig. 1D,E). Buller’s drop is nucleated
9 by the secretion of hygroscopic substances, such as mannitol, that decrease the vapor
10 pressure of the incipient droplet (Webster et al., 1995). In the meantime, a film of water
11 develops on the spore probably following a similar process. When the drop reaches a
12 critical size, it touches the water film on the spore surface. At this point, surface tension
13 quickly pulls the drop onto the spore thus creating the necessary momentum to detach the
14 spore from the sporogenic surface. The spore can then fall freely under the action of
15 gravity. Upon emerging from the cap, the spore is carried away by air currents to a distant
16 location where it can germinate to produce a new mycelium and, ultimately, new
17 mushrooms.

18
19 Surface tension is almost imperceptible at length scales at which humans operate.
20 However, at microscopic length scales, surface tension forces dominate over the force of
21 gravity. This fact can be understood from a simple scaling argument. The force of gravity
22 on an object such as a spore scales as $F_g \sim \rho g R^3$, where ρ is the density of the object, $g =$
23 9.8 m s^{-2} is the gravitational acceleration, and R is the characteristic length of the object.
24 On the other hand, the surface tension force is $F_\gamma \sim \gamma R$ where γ is the liquid’s surface
25 tension ($\gamma = 72 \times 10^{-3} \text{ N m}^{-1}$ for water at room temperature). Considering the ratio of these
26 forces: $F_\gamma / F_g \sim \gamma / \rho g R^2$; it can be seen that as R gets small, the surface tension force
27 becomes increasingly important and dominates the force of gravity for R smaller than 1
28 mm. This simple phenomenon has profound consequences on the release of spores. The
29 dispersal of most fungal spores by wind requires that the spores be small thus making the

1 force of gravity inconsequential compared to adhesion forces. As a result, spores tend to
2 cling to each others and to the gills of mushroom caps. Active spore ejection provides a
3 solution to this problem which explains the great diversity of mechanisms for spore release
4 in fungi and nonvascular plants (Straka, 1962). However, unlike other active dispersal
5 mechanisms which involve mass release of spores from specialized launching structures,
6 ballistospores are *self-propelled* by water.

7
8 Given that a large mushroom can shed spores at the astonishing rate of 40 million
9 spores per hour (Buller, 1950); the release of ballistospores has rightfully attracted some
10 attention (Buller, 1950; Ingold, 1939; Money, 1998). As early as 1939, Ingold determined
11 that the surface energy in Buller’s drop is sufficient to account for the kinetic energy of the
12 spore (Ingold, 1939). He, however, concluded his discussion of the topic remarking that
13 “although there appears to be sufficient surface energy to discharge the spore it is not too
14 easy to see how this energy could be mobilized to bring about discharge” (Ingold, 1939).
15 More recently, Webster and coworkers (Turner & Webster, 1991) were able to predict the
16 initial spore velocity with respectable accuracy based on a few judicious assumptions. The
17 development of highspeed video cameras and their recent application to visualize
18 ballistospore ejection (Pringle et al., 2005) provide, for the first time, a way to address
19 Ingold’s question with direct measurement of all key parameters in the problem.

20
21 Here, we present a detailed analysis of how surface tension is used for spore
22 ejection in *Auricularia auricula* (“tree ears”) and *Sporobolomyces* yeasts. In particular, we
23 quantify the forces and energies of the three stages of the ejection process: the transfer of
24 surface energy from the drop to the spore, the work of fracture required to release the spore
25 from the sterigma, and the kinetic energy of the spore after ejection. Our analysis reveals
26 an exquisite fine-tuning of the different stages that yields a surprisingly high efficiency for
27 the transfer of energy from Buller’s drop to the spore.

1 **Materials and methods**

2 *Specimen preparation*

3 To initiate spore development and spore discharge, dehydrated *Auricularia auricula*
4 fragments were first imbibed on a wet towel and then kept under humid conditions with the
5 fertile surface facing downward. After a few hours, spore ejection had begun as indicated
6 by the presence of white spores on the bottom of the dish. We cut thin vertical sections (0.5
7 mm) of the fungus and laid them flat on a microscope slide covered with a thin (100-200
8 μm) layer of 2% agar. Sterigmas were now oriented horizontally so that spores were
9 ejected perpendicular to the optical axis of the microscope. Spores from yeast-like species
10 were isolated from leaves. Although the yeasts were not identified to the species level, they
11 are members of the Urediniomycetes (the rust fungi), likely of the genus *Sporobolomyces*.
12 The yeasts were plated from a primary culture onto a thin layer of a 2% nutrient agar. After
13 a few days, the spores germinated to form hyphae, sterigmas and new spores. Our yeast
14 cultures may have included more than one species but we found little quantitative
15 differences between the different cultures. Therefore, for simplicity, we are treating all
16 samples as a single taxon. All experiments were performed on *A. auricula* and the yeast
17 species, except for the work of fracture of the hilum which was performed on *A. auricula*
18 only.

20 *Microscopy and imaging*

21 All imaging was done in transmitted light with 20 \times and 40 \times objectives. Images were
22 captured with a Phantom V7.0 or a Photron Ultima APX-RS highspeed camera at a frame
23 rate of up to 250,000 frames per second (fps) and exposure times as short as 1 μs . The high
24 acquisition rate necessary to capture spore ejection can be achieved only when image
25 resolution is low (typically 32 \times 128 pixels). Although our analyses were performed on
26 these raw images, the frames from these time lapse sequences are presented in the figures
27 at higher resolution to improve clarity. We include as supplementary material three movies
28 (AVI format) for *A. auricula*, and one for the *Sporobolomyces* yeasts. The frame rates for
29 the movies are: *Auricularia1.avi* – 90,000 fps; *Auricularia2.avi* – 80,000 fps;
30 *Auricularia3.avi* – 250,000 fps; *Yeast.avi* – 90,000 fps.

1

2 *Spore ballistics*

3 We developed image analysis routines in Matlab (The MathWorks, Natick, MA, USA) to
 4 track the centroid of the spore and the rotation of the spore's major axis over the entire
 5 trajectory. Although spore translation in *A. auricula* and *Sporobolomyces* yeasts could be
 6 tracked reliably in all time lapse sequences, only *A. auricula* offered two spores with
 7 rotation confined to the imaging plane that could thus be analyzed for their angular
 8 velocity. The *Sporobolomyces* yeasts could not be positioned such that the spore trajectory
 9 was confined to the focal plane of the microscope; the spores thus moved quickly out of
 10 focus. To compute the spore velocity, we used a 3D tracking algorithm that relies on the
 11 size of the out-of-focus spore to infer its vertical position. The calibration for the vertical
 12 position was obtained by imaging particles at known vertical displacements above or
 13 below the focal plane and recording the size of the out-of-focus particles.

14

15 As we shall show in the Results section, the Reynolds number for spore ejection is small.
 16 Therefore Stokes' law provides a good description of the drag force acting on the spore
 17 (Happel & Brenner, 1983). Assuming a spherical spore, the ballistic trajectory of the spore
 18 will thus be governed by the following force balance: $D = 6\pi\mu Rv = ma$, where D is the
 19 drag force, R , m , v , and a are respectively the mean radius, mass, velocity and acceleration
 20 of the spore (including the fused drop), and $\mu = 1.84 \times 10^{-5}$ Pa s is the dynamic viscosity of
 21 air. The force balance equation can be rearranged to give:

$$22 \quad \frac{1}{v} \frac{dv}{dt} = \frac{6\pi\mu R}{m}$$

23 Integrating gives $v(t) = V_0 \exp(-t/\tau_T)$, where $\tau_T = m/6\pi\mu R$. We can integrate again to find
 24 the spore position along the axis of discharge (x) assuming that $x(0) = 0$:

$$25 \quad x(t) = V_0 \tau_T (1 - e^{-t/\tau_T}) \quad (1)$$

26 A similar equation can be derived for the viscous dissipation associated with the rotation of
 27 the spore:

$$28 \quad \theta(t) = \Omega_0 \tau_R (1 - e^{-t/\tau_R}) \quad (2)$$

1 where θ is the angular position of the spore, Ω_0 is the initial angular velocity and $\tau_R = m$
 2 $/20\pi\mu R$ is the characteristic decay time for the rotation of the spore (Happel & Brenner,
 3 1983). Equations 1 and 2 were used to fit the observed spore trajectories and infer the
 4 parameters V_0 , Ω_0 , τ_T and τ_R .

5 *Measurement of rupture force*

6 The rupture force of the hilum in *A. auricula* was measured with custom-made
 7 micropipettes calibrated on an analytical balance (0.1 μN precision). Using a
 8 micromanipulator, a micropipette was brought into contact with the top of the spore,
 9 perpendicular to the sterigma. A water film provided adhesion between the spore and the
 10 glass micropipette. In some experiments, we also used poly-L-lysine coated micropipettes
 11 to enhance adhesion. The micropipette was then displaced slowly until the spore detached
 12 from the sterigma or until the adhesion between the spore and pipette failed. The force was
 13 calculated from the deflection of the micropipette with an error of $\pm 5\%$. To infer the
 14 spring constant of the sterigma, we measured its elongation δ just prior rupture (error of
 15 10%).
 16

17 *Surface energy available for spore ejection*

18 The energy available to eject the spore comes from the surface energy stored in Buller's
 19 drop. For *A. auricula*, the surface energy freed during the fusion process (ΔE_p) can be
 20 calculated from the coalescence of a spherical drop onto a plane (Fig. 2A). The energy is
 21 equal to the difference in surface area of the spore-drop system before and after
 22 coalescence, that is:
 23

$$\begin{aligned}
 24 \quad \Delta E_p &= (\gamma_{SV}A_S + \gamma 4\pi R_D^2) - (\gamma_{SL}A_S + \gamma A_D) \\
 25 \quad &= (\gamma_{SV} - \gamma_{SL})A_S + \gamma(4\pi R_D^2 - A_D) \quad (3)
 \end{aligned}$$

26 where γ_{SV} , γ_{SL} , and γ are the energies associated with the spore-vapor, spore-liquid, and
 27 liquid-vapor interfaces, respectively. R_D is the radius of the drop before fusion, A_S is the
 28 area of the spore covered by the drop after fusion and A_D is the drop surface area after
 29 fusion.

Using Young's law for the contact angle ($\gamma_{SV} = \gamma_{SL} + \gamma \cos \theta$) (de Gennes et al., 2003), we have:

$$\Delta E_p = \gamma (\cos \theta A_S - A_D + 4\pi R_D^2)$$

The coalesced drop is a spherical cap of radius R'_D and contact angle θ for which the area is $A_D = 2\pi R_D'^2 (1 - \cos \theta)$, the volume is $\pi R_D'^3 (1 - \cos \theta + (\cos^3 \theta - 1)/3)$, and the projected area onto the spore is $A_S = \pi (R'_D \sin \theta)^2 = \pi R_D'^2 (1 - \cos^2 \theta)$. Then:

$$\begin{aligned} \gamma(A_S \cos \theta - A_D) &= \gamma(\pi R_D'^2 \cos \theta (1 - \cos^2 \theta) - 2\pi R_D'^2 (1 - \cos \theta)) \\ &= -\gamma\pi R_D'^2 (2 - 3 \cos \theta + \cos^3 \theta) \end{aligned}$$

From the conservation of the volume, one can write:

$$4/3\pi R_D^3 = \pi/3 R_D'^3 (2 - 3 \cos \theta + \cos^3 \theta)$$

Therefore, the surface energy available for spore ejection is:

$$\Delta E_p = \gamma 4\pi R_D^2 (1 - R_D/R'_D). \quad (4)$$

As would be expected, ΔE_p is proportional to the total surface area of Buller's drop ($4\pi R_D^2$) times a factor that accounts for the degree of spreading of the drop onto the spore ($1 - R_D/R'_D$). Using the same approach, it is easy to derive the surface energy for the nearly spherical spores of the *Sporobolomyces* assuming that Buller's drop envelops the spore (Fig. 2B).

Error analysis

The main error in our experimental observations comes from the length measurements made on video images. These measurements are used to assess the spore and drop radii and for calculating their volumes. The length measurements were precise to ± 0.5 pixel while the diameter of the drop was < 7 pixels and the spore's dimension were $\sim 8 \times 15$ pixels. As seen in Eq. 4, the prediction of the freed surface energy depends on two length measurements: R_D and R'_D . Prediction of the initial velocity of the spore (V_0) requires in

1 addition the width (W_S) and length (L_S) of the spore. The absolute error on the velocity
 2 estimate (ΔV_0) is given by the following equation:

$$3 \quad \Delta V_0 = \left| \frac{\partial \mathcal{V}_0}{\partial R_D} \right| \Delta R_D + \left| \frac{\partial \mathcal{V}_0}{\partial R'_D} \right| \Delta R'_D + \left| \frac{\partial \mathcal{V}_0}{\partial W_S} \right| \Delta W_S + \left| \frac{\partial \mathcal{V}_0}{\partial L_S} \right| \Delta L_S \quad (5)$$

4 where $\Delta R_D = \Delta R'_D = \Delta W_S = \Delta L_S = 0.5$ pixels are the absolute errors for the length
 5 measurements. Using Eq. 5, we find that the relative error on the predicted velocity is
 6 $\Delta V_0 / V_0 = 22\%$.

7

8 **Results**

9 Spore ejection is best described by first analyzing the spore ballistics to infer the spore
 10 initial velocity and kinetic energy. We then proceed to a mechanical analysis of the stages
 11 that precede ejection.

12

13 *Spore ballistics – the “sporabola”*

14 To quantify the initial velocity and kinetic energy present in the spore at the moment of
 15 ejection, we analyzed the ballistic trajectory of the spore (Fig. 3, see also the movies
 16 available as supporting material). Buller (1950) coined the word “sporabola” to describe
 17 the particular trajectory followed by the spore. The shape of the sporabola results from the
 18 interplay of gravity and viscous forces acting on the spore. The Reynolds number at
 19 ejection is $Re = V_0 L / \nu \approx 0.5$ where L and V_0 are the spore length and spore velocity; and ν
 20 is the kinematic viscosity of air ($1.4 \times 10^{-3} \text{ m}^2 \text{ s}^{-1}$). Given the small Reynolds number,
 21 Stokes law provides a good description of the drag force acting on the spore (Happel &
 22 Brenner, 1983). The spore position along the axis of discharge (x) is thus given by (see
 23 Materials and Methods section):

$$24 \quad x(t) = V_0 \tau_T (1 - e^{-t/\tau_T})$$

25 where V_0 is the initial spore velocity and τ_T is a characteristic decay time due to viscous
 26 drag on the spore translation. The spore rotation, clearly seen in Fig. 3A and D, is also
 27 damped by air viscosity. The angular position is:

$$28 \quad \theta(t) = \Omega_0 \tau_R (1 - e^{-t/\tau_R})$$

1 where Ω_0 is the initial angular velocity and τ_R is a characteristic decay time for the spore
 2 rotation. As shown in Fig. 3, these relations fit the data very well and yield, for the spore
 3 shown in Fig. 3A, an initial velocity of $V_0 = 0.8 \text{ m s}^{-1}$, an angular velocity of $\Omega_0 = 9 \times 10^4$
 4 rad s^{-1} , and decay times of $\tau_T = 184 \mu\text{s}$ and $\tau_R = 66 \mu\text{s}$ (see Table 1 for a summary of the
 5 data). Figure 4 shows spore ejection in a *Sporobolomyces* yeast. For this sequence, the
 6 spore velocity is $V_0 = 1.6 \text{ m s}^{-1}$.

7

8 According to Stokes' law, the decay times are $\tau_T = m_{SD}/6\pi\mu R$ and $\tau_R = m_{SD}/20\pi\mu R$ where R
 9 and m_{SD} are respectively the mean radius and mass of the spore-drop complex, and $\mu =$
 10 $1.84 \times 10^{-5} \text{ Pa s}$ is the dynamic viscosity of air (Materials and Methods; Happel & Brenner,
 11 1983). We can therefore compare the decay times inferred from the fitted spore
 12 displacement in Fig. 3 with those predicted by the theory. For the decay time associated
 13 with the translational velocity (τ_T), the average ratio of measured over calculated time is
 14 0.91 (standard deviation: $\sigma = 0.08$, for $n = 4$ measurements). For the decay time associated
 15 with the angular velocity (τ_R), the average ratio is 1.08 ($\sigma = 0.19$, $n = 2$). The measurements
 16 are therefore in surprising close agreement with the theory.

17

18 Finally, we can look at the kinetic energy of the spore. The translational energy is
 19 $E_K = m_{SD} V_0^2 / 2$ and the rotational energy is $E_R = m_{SD} r_g^2 \Omega_0^2 / 2$ where r_g is the spore's radius
 20 of gyration. The radius of gyration for a prolate spore rotating about its short axis is $r_g =$
 21 $(a^2 + b^2)/5$, where a and b are the minor and major semi-axes of the spheroid. Substituting
 22 values for the sequences shown in Fig. 3, we find $E_K = 2.3 \times 10^{-13} \text{ J}$ and $E_R = 6.3 \times 10^{-15} \text{ J}$.
 23 Therefore, the amount of energy transferred into translation of the spore is at least thirty
 24 times greater than the energy associated with the spore's rotation.

25

26 *Ejection model*

1 We now address the most fundamental question of the ejection mechanism – how the
2 surface energy stored in Buller’s drop is transformed into kinetic energy. To answer this
3 question, we need a proper understanding of the fusion process. Fusion takes place over a
4 time interval of less than $4 \mu\text{s}$ and is therefore just below the temporal resolution of most
5 highspeed cameras currently available. Using a frame rate of 250,000 images per second
6 and a shutter speed of $1 \mu\text{s}$, we obtained some new and critical information about the early
7 stages of spore ejection (Fig. 5). The first frame in Fig. 5A shows the drop that has
8 condensed at the base of the spore. On the second frame, the drop has touched the spore
9 and coalesced. The drop has not spread over the spore completely since its outline can still
10 be discerned. In the third frame, the spore has been ejected while the top border of the drop
11 is still visible on the spore. Finally, the last frame shows the spore rotation in and out of the
12 image plane. This sequence of images establishes that the drop travels only a short distance
13 on the spore and does not spread over the entire surface. Fig. 5B,C offers additional
14 evidence of the partial fusion of the drop which, as we will show, has some important
15 implications for the amount of surface energy available to release the spore.

16 Consideration of the forces acting during the coalescence of Buller’s drop reveals
17 that ballistospore ejection is the fungal equivalent of jumping (Fig. 6). The same three
18 ingredients are present – a lowering of the center of mass, a quick release of energy, and an
19 interaction with a rigid support. Growth of Buller’s drop at the proximal end of the spore
20 lowers the spore’s center of mass (i.e. it brings it closer to the sterigma) as well as provides
21 the energy to be used during ejection. This step is the ballistospore’s way of bending its
22 “legs” in preparation for jumping. As soon as fusion begins, the drop exerts on the spore a
23 surface tension force directed towards itself and the spore exerts on the drop a force of the
24 same magnitude but of opposite direction (Fig. 6A). With no external interaction (isolated
25 system), the drop and spore would move towards each other, and the global center of mass
26 would remain immobile. Thus, there would be no ejection. In the case of ballistospores, the
27 sterigma plays the role of the rigid support. Its presence prevents the spore from moving
28 towards the drop by exerting a reaction force opposing the surface tension force applied by
29 the drop. The sterigma force is the external force acting on the spore-drop complex that
30 leads to the motion of the center of mass. The same requirement for interaction with a rigid

1 support is found in jumping. There, the moments applied at the leg joints must be resisted
 2 by the ground to generate the impulse that will accelerate the center of mass. Ballistospore
 3 ejection, however, differs from jumping in one important way. The spore is not resting on
 4 the sterigma but is attached to it. Therefore, as the spore launches forward, it will put the
 5 sterigma under tension. The latter must break easily to release the spore.

6
 7 This scenario emphasizes the critical role played by Buller's drop and the sterigma
 8 during spore ejection. We can subdivide the ejection process into four stages (Fig. 6).
 9 During the first stage, Buller's drop grows thus lowering the center of mass of the spore
 10 and storing the energy that will be used during ejection. The second stage encompasses the
 11 early coalescence during which the sterigma is under compression and provides the
 12 counter-acting force necessary to move the global center of mass of the spore-drop
 13 complex. It is this force that allows Buller's drop to be accelerated up to a characteristic
 14 speed V_D . In the third phase, the drop decelerates as it transfers its momentum to the spore.
 15 The sterigma is now under tension and needs to break easily to release the spore without
 16 dissipating its kinetic energy. Finally, the fourth stage is the release of the spore.

17
 18 The simplest model for energy transfer suggests that the kinetic energy of the drop
 19 is equal to the difference in surface energy, ΔE_p , between the initial state just before
 20 coalescence and the final state just after coalescence (energy loss will be considered in the
 21 last section). The validity of this assumption can be ascertained by estimating the Reynolds
 22 number for the drop motion. We find $Re = V_D R_D / \nu \approx 50$. The relatively large value for the
 23 Reynolds number confirms that viscous effects are small compared to inertial effects
 24 leading to an efficient transfer of surface energy into kinetic energy. Therefore, we can
 25 write $m_D V_D^2 / 2 = \Delta E_p$, where m_D and V_D are the mass and velocity of the drop
 26 respectively. The latter phase of the coalescence is an inelastic shock between the drop and
 27 the spore. Although the energy is not conserved, the linear momentum is conserved which
 28 implies that $V_0 = m_D V_D / m_{SD}$. This model answers Ingold's question of how the surface
 29 energy stored in Buller's drop is transformed into kinetic energy of the spore.

1

2 *Rupture force of the sterigma*

3 The strength of the chitinous wall of the sterigma could easily exceed the force created by
4 the fusion of Buller's drop. Therefore, to predict the initial velocity of the spore at ejection,
5 the energy required to break the hilum must be known. We measured the rupture force (F_B)
6 by pulling on spores with calibrated glass microcantilevers. The microcantilever was
7 brought in contact with the distal end of the spore and gradually pulled away (Fig. 7,
8 insets). Surface tension between the cantilever and the spore allowed us to put the spore
9 and sterigma under tension. Our measurements reveal two spore classes (Fig. 7). Some
10 spores are weakly attached to the sterigma and are removed with a force between 0.08 and
11 $0.3 \mu\text{N}$ (mean $F_B = 0.15 \mu\text{N}$). Other spores are strongly attached to the sterigma and cannot
12 be removed with forces up to $1.2 \mu\text{N}$ (the maximal force that could be applied with the
13 experimental set-up). For these spores, the force required to fracture the hilum is higher
14 than the adhesion force between the cantilever and the spore. Most attempts to increase the
15 adhesion between the spore and the cantilever, and thus apply higher forces on the hilum,
16 failed; probably because the wet spore surface does not allow strong bonding. However,
17 numerous trials with cantilevers coated with poly-L-lysine yielded a few strongly bonded
18 cantilevers. For these experiments, the hilum either ruptures for forces in the low range
19 observed before or for large forces above $1 \mu\text{N}$ and up to $4.8 \mu\text{N}$ (Fig. 7). The two spore
20 classes provide direct evidence for the development of an abscission zone at spore maturity
21 to allow easy release of the spore (van Neil et al., 1972; McLaughlin et al., 1985). The
22 upper force range gives an estimate of the force required to rupture the hilum before the
23 abscission zone has fully developed.

24

25 For a finite rupture force, the spore velocity is reduced by an amount ΔV that
26 depends on the work done to fracture the hilum. During the late phase of the coalescence
27 process, the sterigma is stretched until the hilar region is fractured. Given a stiffness k and
28 an elongation δ for the sterigma, the elastic force acting on the sterigma is $F_E = k\delta$. When
29 F_E reaches the rupture force F_B , the hilum breaks. The energy needed to sever the

1 attachment is equal to the work done by the elastic deformation: $E_B = F_B^2 / (2k)$. We
 2 measured the stiffness k of the sterigma for different spores with the force experiment
 3 reported in Fig. 7 and found values between 0.45 N m^{-1} and 1.5 N m^{-1} (mean of 0.72 N m^{-1}).
 4). Using our measurements of rupture force and stiffness, we can compute the energy
 5 required to liberate the spores in *A. auricula*. The energy of fracture is $E_B = 1.6 \times 10^{-14} \text{ J}$
 6 and corresponds to a velocity reduction of 3.4%. Therefore, the work of fracture dissipates
 7 only a small fraction of the kinematic energy of the spore. On the other hand, Buller's drop
 8 does not contain enough energy to rupture the hilum before the abscission zone has been
 9 weakened. This observation may explain why, on some occasion, fusion of Buller's drop
 10 fails to release the spore (Buller, 1950).

11 *Transfer of surface energy*

12 The central component of our model is the calculation of the surface energy available to
 13 accelerate the drop. This energy is equal to the difference in surface energy between the
 14 initial state just before coalescence and the final state just after fusion. The exact
 15 expression for the difference in energy depends on spore geometry and final drop
 16 geometry. For *A. auricula*, our observations of the coalescence process (Fig. 5) reveal that
 17 the fused drop adopts a geometry close to a spherical cap. The difference in surface energy
 18 is (see Materials and Methods):
 19

$$20 \quad \Delta E_p = \gamma 4\pi R_D^2 (1 - R_D / R'_D) \quad (6)$$

21 where R_D and R'_D are the radii of the drop before and after fusion. This equation gives a
 22 measure of the energy available to accelerate the drop. Setting the drop kinetic energy
 23 equal to the freed surface energy ($m_D V_D^2 / 2$) and using $m_D = 4\pi\rho R_D^3 / 3$, we find for the drop
 24 velocity:

$$25 \quad V_D \approx \left[\frac{6\gamma}{\rho} (1/R_D - 1/R'_D) \right]^{1/2} \quad (7)$$

26 The expression for V_D takes into account the spore geometry and wettability through R'_D .
 27 Using the conservation of momentum between the drop and spore, it is possible to predict

1 the initial spore velocity V_0 . The prediction for the ejection shown in Fig. 3A is 1.2 m s^{-1}
 2 while the observed velocity is 0.8 m s^{-1} . The ratios of the predicted and observed velocities
 3 for the entire set of experiments are listed in Table 2. The predicted velocity is surprisingly
 4 accurate given that energy loss, either to break the hilum or through dissipation during the
 5 fusion process, has not been taken into account.

6
 7 It is also possible to predict the angular velocity of the spore. A torque is exerted on
 8 the spore since the surface tension force is applied at some distance from the point of
 9 contact between the spore and the sterigma (Fig. 6A). This torque explains the rotation of
 10 the ejected spore. Using the conservation of angular momentum (Happel & Brenner,
 11 1983), we have $m_D V_D l = m_{SD} r_g^2 \Omega_0$ where l is the distance between the global center of
 12 mass and the point of drop fusion and r_g is the radius of gyration of the spore-drop
 13 complex. For the discharge shown in Fig. 3A, $l \approx 3 \mu\text{m}$ giving a calculated angular velocity
 14 of $\Omega_0 \approx 8 \times 10^4 \text{ rad s}^{-1}$, in good agreement with the measured value of $9 \times 10^4 \text{ rad s}^{-1}$. We
 15 have not been able to investigate this aspect of the discharge further because the rotation of
 16 most spores was not confined to the imaging plane and thus could not be measured.

17
 18 In the *Sporobolomyces* yeasts, the spore is nearly spherical and is covered by a film
 19 of water (Fig. 4). The fusion is thus close to the coalescence of a drop of radius R_D onto a
 20 perfectly wetting spherical spore of radius R_S . The difference in surface energy is then:

$$21 \quad \Delta E_p = \gamma 4\pi(R_D^2 + R_S^2 - R_D'^2) \quad (8)$$

22 where $R_D' = (R_D^3 + R_S^3)^{1/3}$. Equating the surface energy and the drop kinetic energy and
 23 solving for the drop velocity, we find:

$$24 \quad V_D \approx \left[\frac{6\gamma}{\rho R_D^3} (R_D^2 + R_S^2 - R_D'^2) \right]^{1/2} \quad (9)$$

25 Using this equation and the conservation of momentum, we predict a velocity $V_0 = 3.4 \text{ m}$
 26 s^{-1} while the observed velocity is 2.3 m s^{-1} . Given that some energy is necessarily lost in
 27 the coalescence process and in breaking the hilum, the agreement is again very good.

1

2 *A test of the model*

3 The key assumption of our model is that the drop reaches a characteristic velocity V_D that
4 can be predicted from the change in surface energy of the system. To test the validity of
5 this assumption, we performed experiments on an artificial system that mimics the fusion
6 of Buller's drop. A drop was placed on a highly hydrophobic plate while another plate, this
7 one wettable, was approached slowly from above until it touched the drop. Contact with
8 the wettable plate induced a fast upward motion of the drop (Fig. 8). The contrast of
9 wettability between the two substrates was such that the drop moved in its entirety from
10 the lower surface to the upper one. This coalescence process is very similar to what
11 happens when a drop wets the spore. Bianche and coworkers (2004) performed a similar
12 experiment but with plates of similar wettability, leading to a final state where the drop is
13 split between the two surfaces. They provided a scaling relation for the horizontal growth
14 dynamics of the neck. Here, we complement their analysis with a study of the vertical
15 motion of the center of mass.

16

17 We found that after a brief acceleration, the drop's center of mass moves upward at a
18 constant speed (Fig. 8H). Therefore, the fusion process is associated with a characteristic
19 velocity of the center of mass. We measured this characteristic velocity in a series of
20 experiments and plotted it as a function of the theoretical velocity predicted from Eq. 7
21 (Fig. 8I). The observed drop velocity is proportional to the predicted velocity, with a
22 proportionality constant $\beta = 0.28$. The parameter β is a measure of the efficiency of the
23 transfer of surface energy to kinetic energy. The value of β below one indicates that a
24 fraction of the surface energy is lost in the coalescence process and therefore not available
25 to accelerate the drop. By the same token, we can interpret the velocity ratios listed in
26 Table 2 as a measure of the efficiency of the energy transfer in the ballistospores. *A.*
27 *auricula* and the *Sporobolomyces* yeasts show a similar efficiency with more than two
28 third of the surface energy liberated contributing to the kinetic energy of the spore.

29

30 **Discussion**

1 The use of surface tension by ballistosporic fungi offers a new paradigm for performing
2 work at the micron scale. One clear advantage of this mechanism is that work, being
3 performed by the fusion of a water droplet, comes virtually for free. It is only under this
4 condition that the innumerable spores contained in a mushroom cap can all be equipped
5 with their own discharge apparatus. The ballistosporic mode of dispersal is in sharp
6 contrast with the mass release of spores or propagules by specialized launching structures
7 found in other taxa (Straka, 1962). It is therefore of great interest to uncover the design
8 principles that make surface tension an effective source of energy.
9

10 As first stated by Ingold (1939), the key step for ballistospore release is the transfer
11 of surface energy stored in Buller's drop to the spore. Our analysis emphasizes the critical
12 role played by the sterigma. First, during the early phase of the coalescence process, the
13 sterigma provides the external force that prevents the spore from moving toward the drop.
14 The global center of mass of the spore-drop complex is thus projected forward leading to
15 ejection. In the late phase of the coalescence process, the sterigma is now put under tension
16 and should fracture easily to prevent dissipation of the spore energy. Our measurements of
17 the force required to release the spore from the sterigma show that an active weakening of
18 the hilum takes place before ejection. The characteristic rupture force of $0.15 \mu\text{N}$ ($n = 15$)
19 recorded for a weakened hilum is comparable to the rupture force of $0.1 \mu\text{N}$ reported for
20 wind-dispersed fungal conidiospores (Aylor, 1975). This value is large compared to the
21 gravitational force acting on the spore ($F_g \approx 2 \times 10^{-6} \mu\text{N}$) but small compared to the surface
22 tension force that can be exerted by a drop at this scale ($F_\gamma = \gamma 2\pi R_D \approx 1.4 \mu\text{N}$, where $R_D =$
23 $2.25 \mu\text{m}$ is the drop radius). On the other hand, a force of up to $4.8 \mu\text{N}$ is necessary to
24 detach an unweakened spore (Fig. 7), that is, three times the surface tension force.
25 Therefore, without an active weakening mechanism, spore ejection would be impossible.
26

27 To predict the initial velocity of the spore, we developed a model that focuses on
28 the surface energy freed during the coalescence process. This model predicts with
29 surprising accuracy the initial translational and angular velocity of the spore, particularly if

1 one makes allowance for energy dissipation during fusion. A prediction of the model is
 2 that the geometry of the *fused drop* affects the amount of energy available to eject the
 3 spore. Consequently, spore morphology and the wetting properties of the spore surface can
 4 play an important role in the transfer of surface energy to kinetic energy. The low
 5 efficiency of energy transfer in our artificial system when compared to ballistospores
 6 (Table 2) also emphasizes the challenges associated with the fine-tuning of such a
 7 mechanism. It is likely that the difference in scale between the two systems explains the
 8 higher efficiency for ballistospore ejection. It is also noteworthy that our model predicts
 9 similar efficiency of energy transfer for the two species studied despite differences in spore
 10 geometry and a three fold difference in the initial velocity between the *Sporobolomyces*
 11 and *A. auricula* spores.

12
 13 A way to evaluate viscous loss is to calculate the energy loss in volume during the fusion
 14 process. This energy can be written $E_V = T_D \mu \int \xi^2 dV$. $T_D \sim R_D/V_D$ is the characteristic time
 15 for the drop merging process and ξ is the shear rate. By taking a characteristic shear rate
 16 $\xi \sim V_D/R_D$ due to the small deformation of the drop, the integration gives $E_V \approx 4\pi\mu R_D^2 V_D/3$.
 17 Hence the ratio between viscous energy loss and the surface energy of the drop is: $E_V/E_p =$
 18 $E_V/4\pi\gamma R_D^2 \sim \mu V_D/3\gamma = Ca/3 \sim 1/20$. The energy ratio corresponds to the capillary number
 19 (Ca). Here this ratio is much smaller than one, indicating small viscous loss.

20
 21 We have found it useful to compare ballistospore release with jumping in animals.
 22 We first note that the take-off velocity of the spore (1 to 2 m s^{-1}) falls precisely within the
 23 narrow range of take-off velocities (<1 to 4 m s^{-1}) reported for good jumpers from insects
 24 to mammals (Vogel, 2005a; Vogel, 2005b). This striking observation suggests that a take-
 25 off velocity on the order of 1 m s^{-1} is a fundamental limit for jumpers whether they achieve
 26 this velocity through muscle work or surface tension. Vogel (2005b) posited that the
 27 strength of biomaterials may impose limits on the stress that can be applied to accelerate
 28 jumpers and thus may set the maximal take-off velocity. However, it is doubtful that the

1 same argument would apply to ballistospores. As we have shown, the surface tension force
2 exerted by Buller's drop is $F_\gamma = 1.4 \mu\text{N}$ and is applied on a cross-section of $5 \mu\text{m}^2$, which is
3 a level of stress that most biomaterials can sustain.

4
5 In both insects and vertebrates, the velocity of the center of mass is known to increase
6 monotonically during the active part of the jump up to the take-off velocity (Burrows,
7 2006; Burrows, 2008; Marsh & Johnalder, 1994). The evolution of the center of mass
8 velocity can be accounted for if a finite force is applied during the entire hind limb
9 deployment. By analogy, it would be tempting to assume that the velocity of Buller's drop
10 in ballistospores follows a similar evolution with surface tension, instead of muscle work,
11 providing a roughly constant force over the entire distance traveled by the drop. However,
12 as can be seen in our artificial system (Fig. 8H), this approach would lead to a gross
13 overestimate of the drop velocity. The drop is in fact accelerated over a very short distance
14 and then displaced at a constant characteristic velocity. We have argued that understanding
15 what sets this characteristic velocity is the key to predicting the spore velocity at ejection.
16 Our results show that the characteristic velocity scales with the surface energy freed during
17 the coalescence (Fig. 8I) and thus highlight the importance, in ballistospores, of the final
18 geometry of Buller's drop in determining the energy available for discharge and the take-
19 off velocity of the spore.

21 **Acknowledgments**

22 We would like to thank the MRSEC at Harvard University and D.A. Weitz for funding; B.
23 Roman, L. Mahadevan, D. Quéré, and H.A. Stone for useful comments on the manuscript;
24 as well as D.H. Pfister, N.M. Holbrook and M.A. Zwieniecki for help with the
25 experiments.

1 **References**

- 2 Aylor, D. E. (1975). Force required to detach conidia of *Helminthosporium maydis*. *Plant*
3 *Physiol.* 55, 99–101.
- 4 Biance, A., Clanet, C. & Quéré, D. (2004). First steps in the spreading of a liquid droplet.
5 *Phys. Rev. E* 69, 016301.
- 6 Buller, A. (1909-1950). *Researches on fungi.*, vol. 1-7,. Longmans, Green and Company.
- 7 Burrows, M. (2006). Jumping performance of froghopper insects. *J. Exp. Biol.* 209, 4607–
8 4621.
- 9 Burrows, M. (2008). Jumping in a wingless stick insect, *Timema chumash* (phasmatoidea,
10 timematodea, timematidae). *J. Exp. Biol.* 211, 1021–1028.
- 11 de Gennes, P., Brochard-Wyart, F. & Quéré, D. (2003). *Capillarity and Wetting*
12 *Phenomena: Drops, Bubbles, Pearls, Waves.* Springer Verlag.
- 13 Happel, J. & Brenner, H. (1983). *Low Reynolds number hydrodynamics.* Springer Verlag.
- 14 Ingold, C. (1939). *Spore discharge in land plants.* Oxford University Press.
- 15 Marsh, R. L. & Johnalder, H. B. (1994). Jumping performance of hylid frogs measured
16 with high-speed cine film. *J. Exp. Biol.* 188, 131–141.
- 17 McLaughlin, D., Beckett, A. & Yoon, K. (1985). Ultrastructure and evolution of
18 ballistosporic basidiospores. *Bot. J. Linn. Soc.* 91, 253–271.
- 19 Money, N. (1998). More g's than the space shuttle: ballistospore discharge. *Mycologia* 90,
20 547–558.
- 21 Pringle, A., Patek, S., Fischer, M., Stolze, J. & Money, N. (2005). The captured launch of a
22 ballistospore. *Mycologia* 97, 866–871.
- 23 Straka, H. (1962). Nicht durch Reize ausgelöste Bewegungen vol. 17, of *Handbuch der*
24 *Planzenphysiologie* pp. 716–835. Springer Verlag.
- 25 Turner, J. & Webster, J. (1991). Mass and momentum transfer on the small scale: how do
26 mushrooms shed their spores? *Chem. Eng. Sci.*, 46, 1145–1149.
- 27 van Neil, C., Garner, G. & Cohen, A. (1972). On the mechanism of ballistospore
28 discharge. *Arch. Mikrobiol.*, 84, 129–140.
- 29 Vogel, S. (2005a). Living in a physical world -ii. the bio-ballistics of small projectiles. *J.*
30 *Biosci.*, 30, 167–175.

- 1 Vogel, S. (2005b). Living in a physical world -iii. getting up to speed. *J. Biosci.*, 30, 303–
2 312.
- 3 Webster, J., Davey, R., Smirnoff, N., Fricke, W., Hinde, P., Tomos, D. & Turner, J.
4 (1995). Mannitol and hexoses are components of buller's drop. *Mycol. Res.*, 99, 833–
5 838.
6

1 Table 1: Summary of key measurements

Parameter ¹	<i>Auricularia</i>	<i>Sporobolomyces</i>
<i>Spore:</i>		
Mass (m_S)	2.8×10^{-13} kg	1.5×10^{-13} kg
Radius of gyration (r_g)	3.1 μ m	2.2 μ m
Trans. velocity (V_0)	0.8 m s ⁻¹	2.3 m s ⁻¹
Angular velocity (Ω_0)	7.1×10^4 rad s ⁻¹	NA
Trans. kinetic energy (E_K)	2.3×10^{-13} J	6.7×10^{-13} J
Rot. kinetic energy (E_R)	6.3×10^{-15} J	NA
Rupture force (F_B)	0.15 μ N	NA
<i>Drop:</i>		
Mass (m_D)	4.9×10^{-14} kg	1.2×10^{-13} kg
Radius (R_D)	2.25 μ m	3 μ m
Final radius (R'_D)	5.65 μ m	NA

2

3 ¹ all averages are based on at least five replicates except for the angular velocity and the
 4 rotational kinetic energy which are based on two measurements.

5

1 Table 2: Ratio of the measured (V_0) and predicted (\hat{V}_0) initial spore velocity. Mean values
 2 are reported with their standard deviations (σ) and sample size (n).

Species	V_0 / \hat{V}_0	σ	n
<i>Auricularia</i>	0.73	0.13	5
<i>Sporobolomyces</i>	0.68	0.12	5
<i>Drop-plane system</i> ¹	0.28	0.02	11

3 ¹ based on the ratio of the observed and predicted drop velocities

4
 5
 6
 7

1 Figure 1: Ballistospore discharge in basidiomycetes. (A) Section of a typical mushroom
 2 cap showing the gills and the location of the spore-bearing basidia (insert). The
 3 approximate trajectory of the spore is shown as a dash line (B) A typical basidium with
 4 four spores. (C) Structure of the lower half of the spore (based on McLaughlin et al. 1985).
 5 (D) Spore ejection in *Auricularia auricula*. In this species, spores are borne singly on the
 6 sporogenic surfaces. (E) Diagrammatic representation of the ejection in (D).

7

8 Figure 2: (A) Spore and drop geometry for *Auricularia auricula*. (B) Spore and drop
 9 geometry for the *Sporobolomyces* yeasts.

10

11 Figure 3: Spore ballistics in *Auricularia auricula*. A) Spore trajectory (frame rate: 90,000
 12 fps, shutter: 2 μ s) (see movie Auricularia1.avi as supporting material). Spore position (B)
 13 and rotation angle (C) versus time for the sequence shown in (A). The data points are fitted
 14 with the displacement equation derived from Stokes Law. (D) Spore trajectory (frame rate:
 15 80,000 fps, shutter: 2 μ s) (see movie Auricularia2.avi as supporting material). Spore
 16 position (E) and rotation angle (F) versus time. As above, the data points are fitted with the
 17 displacement equation derived from Stokes' Law. In this example, the rotation of the spore
 18 is not fully confined to the imaging plane which explains the slight deviation of the
 19 observed angular position from the theory (F).

20

21 Figure 4: Spore ejection in a *Sporobolomyces* yeast. In the first frame, the drop is seen to
 22 the left of the spore.

23

24 Figure 5: Early stages of spore discharge in *A. auricula*. It can be seen from these frames
 25 that the drop does not spread completely over the spore (see also movie Auricularia3.avi in
 26 the supporting material). The frame rates and shutter times are respectively: (A) 250,000
 27 fps and 1 μ s; (B) 100,000 fps and 2 μ s; (C) 75,000 fps and 4 μ s.

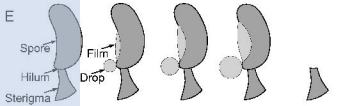
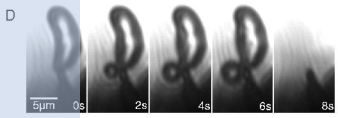
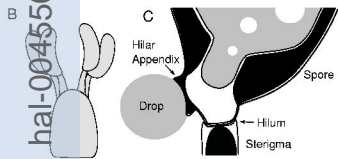
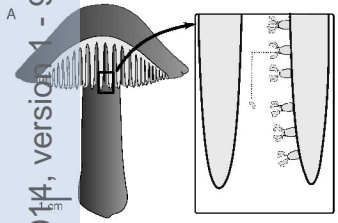
28

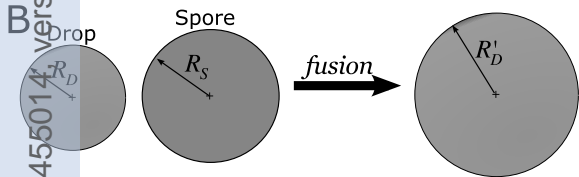
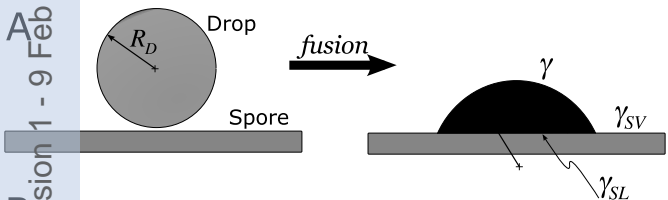
29 Figure 6: (A) The four stages of ballistospore ejection. First, the growth of the drop brings
 30 the center of mass of the spore-drop complex closer to the end of the sterigma. Second, at

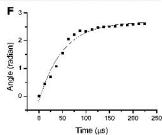
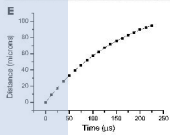
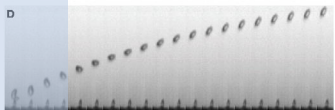
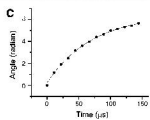
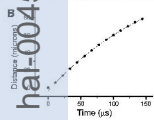
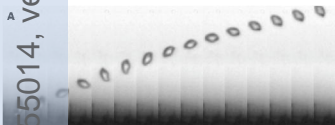
1 the start of the coalescence process, the drop and spore exerts on it each other forces of
 2 equal magnitude but opposite direction (F_D and F_S). The expected downward displacement
 3 of the spore is prevented by the presence of the sterigma giving rise to a reaction force F_{St}
 4 acting at the hilum. Third, in late coalescence, the momentum of the drop is transferred to
 5 the spore which was immobile until then. The transfer of momentum is equivalent to a
 6 force F_{SD} applied at the center of mass of the spore-drop complex. This force puts the
 7 hilum under tension which provides a counteracting force that cannot exceed the fracture
 8 force F_B . Fourth, the hilum is fractured thus releasing the spore. (B) The corresponding
 9 stages in jumping. First, the center of mass is lowered to allow the legs to do work on the
 10 substratum. At this stage, the gravitational force (F_G) and the ground reaction force (F_R)
 11 are balanced. Second, as the legs unfold, the moments at the joints (M) are resisted by the
 12 substratum thus providing the impulse (I) necessary to accelerate the center of mass. Third,
 13 late in the jump, the fast-moving upper body starts to entrain the legs which to this point
 14 were moving slowing upward. Fourth, after take-off all body parts are moving at similar
 15 speeds and only gravity acts on the body.

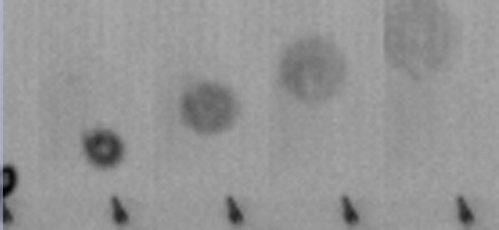
16
 17 Figure 7: Rupture force measurements. The abscissa gives the maximal force recorded at
 18 the time of failure which involved either a fracture of the hilum (top histogram) or an
 19 adhesion failure between the spore and the pipette (bottom histogram). The distribution
 20 indicates two broad classes of spores: weakly attached spore with rupture force $\leq 0.4 \mu\text{N}$
 21 and strongly attached spores that could not be detached with forces of up to $1.2 \mu\text{N}$.
 22 Arrows indicate the hilum rupture force recorded in a second series of experiments with
 23 cantilevers coated with poly-L-lysine.

24
 25 Figure 8: Coalescence of a drop ($R_D = 400 \mu\text{m}$) onto a wettable plate. (A)-(G) Image
 26 sequence of the coalescence process. (H) The position of the drop's center of mass is
 27 plotted as a function of time. The letters correspond to the frames above. (I) Velocity of the
 28 drop center of mass as a function of the predicted velocity $V_D = [(6\gamma/\rho)(1/R_D - 1/R'_D)]^{1/2}$.
 29 The slope of the relation is $\beta = 0.28$ ($R = 0.95$).









10 μm

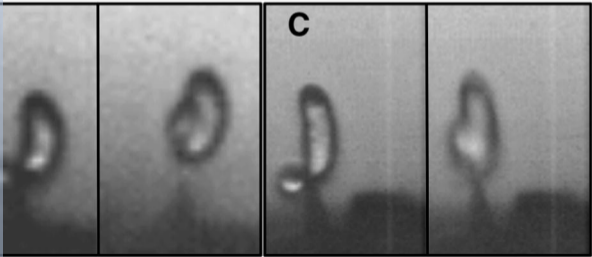
0 μs

4 μs

8 μs

12 μs

C



B

